IEEE Access
Multidisciplinary | Rapid Review | Open Access Journal

Received January 3, 2020, accepted January 12, 2020, date of publication January 17, 2020, date of current version January 27, 2020.

Digital Object Identifier 10.1109/ACCESS.2020.2967065

Low-Complexity Beam Selection Scheme for High Speed Railway Communications

RUI JIANG[1], JIAQI ZHAO[1], YOUYUN XU[1], (Senior Member, IEEE), XIAOMING WANG[1], (Member, IEEE), AND LI ZHANG[2]

[1]College of Telecommunications and Information Engineering, Nanjing University of Posts and Telecommunications, Nanjing 210023, China
[2]College of Computer Science and Technology, Nanjing Forestry University, Nanjing 210037, China

Corresponding author: Youyun Xu (yyxu@njupt.edu.cn)

This work was supported in part by the Grants from the National Key Research and Development Program of China under Contract 2016YFE0200200, in part by the National Natural Science Funds of China under Contract 61601243, Contract 61801240, and Contract 61701253, in part by the Natural Science Foundation of the Jiangsu Providence under Grant BK20180753, and in part by the Research Foundation of Nanjing University of Posts and Telecommunications under Grant NY220008.

ABSTRACT Large-scale multiple input multiple output (MIMO) assisted beamforming based on millimeter waves is an effective way to increase system capacity and data transmission rate for high speed railway (HSR) communication systems. To reduce the number of handovers and improve system throughput, multi-stream beamforming with different beamwidths is used as the transmit beam at the base station (BS). However, when the train moves toward the cell edge, the inter-beam ambiguity (IBA) between multiple beams becomes more and more serious, and the performance of the system will decrease significantly if multiple beams are still activated simultaneously. In order to overcome such difficulty, a low-complexity beam selection scheme based on multi-stream beamforming is proposed in this paper. With this methodology, when the train is in the vicinity of the BS, all beams are activated to achieve the performance of high throughput. Neverthless, when the train moves at the cell edge, only one beam is activated due to the insupportable IBA. The optimal beam switching position could be calculated according to the requirements of the angular resolution. Observing from the theoretical analysis and the simulation results, the proposed scheme can achieve low complementation complexity with high throughput performance.

INDEX TERMS High speed railway, large-scale MIMO, millimeter wave, multi-stream beamforming, beam selection.

I. INTRODUCTION

A rapidly growing demand of high-quality communications is triggered by the booming development of high-speed railway (HSR) [1], [2]. Numerous scholars are committed to the research of HSR communications for the purpose of improving the quality of communication services. In order to meet the demands for high system capacity and high data rate, millimeter waves (mmWave) band covered by 5G communications, should be exploited [3]. However, the mmWave signals with higher frequency will experience severe path loss [4]. Beamforming techniques with massive multiple input multiple output (MIMO) can be used to overcome this difficulty. Massive MIMO using large number of antenna elements, which can service many mobile terminals at the same time to enhance the system throughput and reliability, is one of the key technologies for 5G communications [5], [6].

The associate editor coordinating the review of this manuscript and approving it for publication was Haipeng Yao.

In addition, the line-of-sight (LOS) path of HSR communications is strong, and multi-stream beamforming can be used in this environment to obtain multiplexing gain for further improving system throughput. As the number of the base station (BS) antenna elements increases, the high angular resolution and antenna gain can be achieved [7].

Many issues such as high Doppler shift, frequent handovers and the estimation of the fast time-varying channel [8] should be taken into consideration in the HSR communication systems. Fortunately, there are many feasible methods to solve these problems. The most commonly used method of overcoming the Doppler shift is Doppler diversity, which can improve the received signal to noise ratio and reduce the bit error rate of the received signal [9]–[11]. The dual-link soft handover [12], [13] and dual-link seamless handover [14], [15] are usually applied to increase the probability of successful handover. In order to obtain the accurate estimation of the fast time-varying channel, [16] proposed a MIMO channel estimation using a special frequency division pilot,

which can obtain high precision channel estimation. It's also worth mentioning that some inherent characteristics of HSR communications, such as predictable train position and speed information offered by communication-based train control system [17], can be used to assist in solving these problems.

In HSR communications, many of the current schemes are devoted to single-stream beamforming. In these schemes, only one mobile relay (MR) is served by one beam at one point, which limits system throughput. On the contrary, multi-stream beamforming, which uses multiple beams formed by the BS to simultaneously serve multiple MRs, can improve data transfer rates and transmission reliability significantly. Beamforming concentrates the energy of the signal in the direction of the receiver, thus improving spectrum utilization efficiency. Beamforming design in mmWave communication is critical for large-scale MIMO-assisted multi-stream beamforming to increase system throughput. The current work focuses on two sorts of beamforming techniques which are beam tracking and beam switching. The beam tracking refers to the use of beams to track mobile users based on terminal mobility, which is highly flexible. In [18], a broad beamforming approach is proposed to track the moving users based on the velocity and location information of moving users, which can improve the received signal to noise ratio. However, this method is performed periodically for successive adjacent moving regions of interest, which increases the complexity of the system. A dynamic mmWave beam tracking by jointly adjusting the beam direction and beamwidth is researched in [19]. This scheme converts the problem into non-convex, which can achieve near-optimal throughput performance, but it brings beam adjustment overhead. The beam switching is used to switch the beam from the current serving beam to a better predefined beam based on train position and velocity information, which has low system complexity. Reference [20] proposed a beamforming scheme for off-line calculation of beamforming weights based on location, which can reduce system implementation complexity. However, an extra guard angle is not considered when calculating the beam width, so that the beam width calculation is inaccurate and the success probability of beam switching is reduced. Reference [21] proposes an optimal non-uniform stable beamforming under an iterative redundant network structure to guarantee the reliability of transmission. However, only one optimal beam in one network is used to transmit signals at a time, which limits the transmission rate of the system. Reference [22] proposed a stable beamforming with C/U-plane decoupled structure, using long-term transmit beam and short-term receive beam, which can reduce the number of beam switching. However, only one beam transmits the signals in this paper, which limits the system capacity. In massive MIMO communications, many articles have studied multiple beams for multiple users. Reference [23] proposed a suboptimal low-complexity beam allocation algorithm in multi-user massive MIMO system. This scheme can achieve nearly optimal total data rate and reduce complexity. Reference [24] proposed a greedy algorithm and considered the problem of interference between beams to maximize the sum of data rates and ensure fairness among users for multi-user massive MIMO system. The advantages of multiple beams in massive MIMO communications make it necessary to be researched in HSR communications.

A mmWave-based adaptive multi-beamforming scheme for HSR communication is proposed in [25]. In this method, multiple beams with different beamwidth are applied to increase system capacity. To further optimize the performance of the algorithm, the interference inter the beams is also taken into account. When multiple beams are employed, the inter-beam ambiguity (IBA) becomes larger and larger as the train runs toward the edge of the cell. In order to eliminate the influence of IBA in the multi-stream beamforming, the optimal activated beams should be constantly adjusted to accommodate the changing of train position. Through this scheme, the throughput of HSR communications could be improved dramatically and the outage probability is decreased as well. However, this method requires traversal searching to obtain the optimal activated beams, which is a computationally expensive task and also limits the real-time application. Aiming at the drawbacks of this method, a low-complexity beam selection scheme based on multi-stream beamforming is proposed for HSR communications. In this scheme, the working states of the activated multiple beams are classified into two kinds: one is all the multiple beams activated; the other is only one beam activated. With the predictable position information of the train, the angular resolution of a large-scale antenna array is utilized to choose optimal working state. With this presented methodology, the computational cost of the proposed autofocus algorithm can be reduced effectively via avoiding the procedures of traversal searching. The simulation experiments verify the performance of our methods in terms of the system throughput, the computational complexity and communication outage probability.

The rest of this paper is organized as follows. Section II introduces the system model of HSR communications. Then, section III briefly describes the process of calculating multi-beam width and the adaptive beam adjusting algorithm of the previous scheme. Section IV proposes a low-complexity beam selection scheme, describes its algorithm, and analyzes its complexity. Finally, the performance simulation analysis is given in section V, while section VI concludes the paper.

II. SYSTEM MODEL

For the purpose of improving the throughput in HSR communications, the multi-stream beamforming structure in [25] is applied. The multi-stream beamforming system model for HSR communications is shown in Fig. 1. The roadside BS is equipped with a uniform linear array (ULA) in which N_T antenna elements are deployed linearly, and the radius of the coverage area is R. The BS simultaneously forms a plurality of transmit beams with different widths for serving many MRs. Wide beams can be used to cover wide areas due to less serious path loss in the vicinity of the BS, which

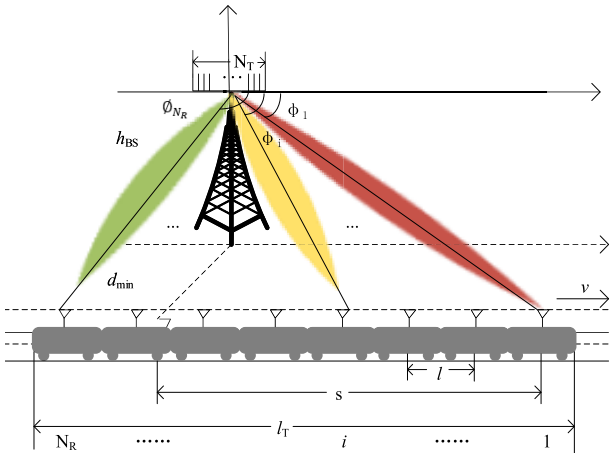

FIGURE 1. Multi-stream beamforming system model for HSR communications.

can extend the service time and reduce the number of beam switching. Narrow beams are used in the edge region of the cell, which has a high beamforming gain to combat path loss. The projection point of the BS on the ground is the coordinate origin O and the train moves from the origin to the edge of the cell along the direction of velocity as shown in Fig. 1. The spacing between adjacent antenna elements is $\Delta_T\lambda$, where Δ_T is the normalized antenna element spacing and λ is the carrier wavelength. The vertical distance between the BS and the railway track is represented as d_{min}, the heights of BS and MRs are h_{BS} and h_{MR}, respectively, ϕ_i indicates the direction of arrival (DOA) from the BS to the ith MRs. In order to overcome the penetration loss of the carriage and mitigate many simultaneous group handovers, a two-hop structure is adopted [26], [27]. This structure divides the communication link into two parts, one is the link between the BS and the MR, and the other is the link between the MR and the passengers in the train. Since the communication between the MR and the passengers is relatively fixed, only the communication between the BS to the MR is considered in multi-stream beamforming design. In mmWave communications, the receiver can also be equipped with a uniform antenna array to form receive beam. It is assumed that there are N_R MRs. An MR equipped with many antennas is installed on the top of each carriage and the distance between adjacent MRs is l. The receiver can automatically adjust the receive beam according to the channel state information. We denote the MR in the head of the train is the first MR and the index number of the remaining MRs increases in the opposite direction of velocity v.

III. ADAPTIVE BEAM ADJUSTING ALGORITHM

Before the adaptive beam adjusting algorithm is performed, multiple beams are formed first. A simple process of calculating multi-beam width is as follows. Suppose that the current transmit beam width received by the ith MR at point k is $\theta_i(k)$. The BS forms a beam as wide as possible to extend the coverage, so the current beam width $\theta_i(k)$ is set to the maximum beam width θ_{max}. The receiver is checked whether the receiving threshold is reached. If it is reached, let $\theta_i(k)$ is the transmit beam width at that point. If not, the beam width is reduced to form a new beam width, which is judged whether it is smaller than the minimum beam width θ_{min}. If it is true, the new beam width is set to the minimum beam width. Otherwise, the receiver is calculated whether it reaches the receiving threshold under the new beam width. The process is repeatedly performed to calculate the beam widths for all MRs in the cell coverage. The BS allocates the obtained beam width to each MR. However, there is interference between multiple beams, and the activated beams need to be adjusted.

An adaptive beam adjusting algorithm based on multi-stream beamforming is proposed in [25] to maximize the throughput of the system. The scheme in [25] is called the previous scheme in this paper. In the previous scheme, the optimal throughput is calculated according to the optimal activated beam set, which was determined by the traversal searching algorithm described as follows.

Algorithm 1 Adaptive Beam Adjusting Algorithm

Input:
$C_{max} = 0, B = \varnothing, B_{opt} = \varnothing, \Omega = \{1, 2, \ldots, N_R\}$
for $k = 1 : N_R$ **do**
  for $i \in \Omega$ **do**
    $B_{opt} = B \cup \{i\}$
    Calculate the total throughput for the active subset B_{opt}:
    $C_i = \sum_{i \in B_{opt}} B \log_2(1 + SINR_i)$
  end for
  $C(k) = \max_{i \in \Omega} C_i$
  $S(k) = \arg\max_{i \in \Omega} C_i$
  $\Omega = \Omega - S(k)$
  $B = B \cup S(k)$
  $k = k + 1$
end for
$C_{max} = \max(C(k))$
$B = \arg\max_{S(k)}(C(k))$
Output: C_{max}, B

Let Ω denotes the candidate beam set and B is the optimal activated beam set. C_{max} refers to the maximum system throughput. The procedure of traversal searching algorithm for the previous scheme is listed in Algorithm 1. Firstly, the maximum throughput $C(1)$ of only one beam is calculated, and the corresponding activated beam set $S(1)$ can be obtained. Then, the maximum throughput $C(2)$ of two beams is calculated and the activated beam set $S(2)$ of two beams can be found. According to the same rule, the maximum throughput $C(N_R)$ of N_R beams can be calculated and the activated beam set $S(N_R)$ of N_R beams can be obtained. Finally, the one with the highest throughput can be found

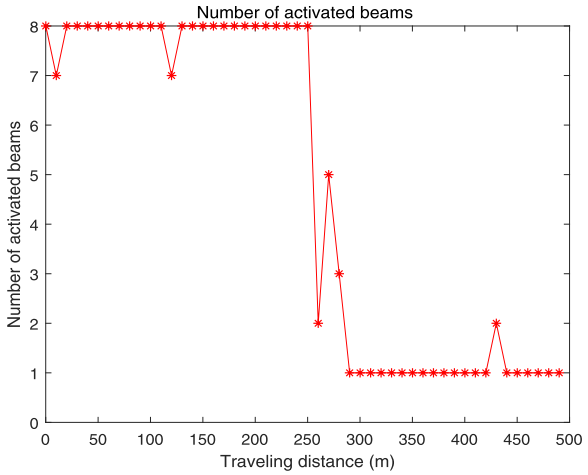

FIGURE 2. The number of activated numbers in previous scheme.

from the $C(k), k \in [1, 2, \ldots, N_R]$, and the corresponding optimal activated beam set $S(k)$ can also be obtained.

Taking 8 MRs as an example, Fig. 2 shows the optimal activated multiple beam situation obtained by traversal searching algorithm in previous scheme. It is observed from Fig. 2 that the number of activated beams near the BS is almost maintained at 8. As the train moves to the cell edge, the number of activated beams will be suddenly lower for maintaining a higher throughput. When the train arrives at the cell edge area, only one beam is activated for serving one MR due to unacceptable interference inter multiple beams. Unfortunately, this process was implemented by a traversal searching algorithm, which undoubtedly increases the computational cost. The more MRs are, the more iterative searches become, the higher the computational cost is.

IV. A LOW-COMPLEXITY BEAM SELECTION SCHEME BASED ON MULTI-STREAM BEAMFORMING

In this section, a low-complexity beam selection scheme based on multi-stream beamforming is proposed. Note that the number of the activated multiple beams goes from 8 to 1 very quickly in Fig. 2. According to the changing regularity, the working state of the activated multiple beams are classified into two kinds: one is all the multiple beams activated; the other is only one beam activated. In our proposed scheme, all the beams are activated to transmit signals in the vicinity of the BS and when the train runs from the center of the cell to the edge of the cell to a certain position s', only one beam is activated due to the unacceptable IBA. s' divides $(0, R]$ into 2 regions, which are $(0, s']$ and $(s', R]$. Thus, the problem of multi-stream beamforming design is translated into finding the optimal switching position of the two kinds of the working state.

A. MATHEMATICAL ANALYSIS

Assuming that the train runs through the entire cell at a constant speed v, the cell is divided into two areas in order to ensure the transmission performance. All beams are activated for transmitting signals in the area near the center of the cell, and only one beam is activated for serving one MR in the area of the cell edge. The switching position of the working states of the two activated multiple beams is determined by the train running to a certain location s' calculated by the inter-beam resolution requirements. For the proposed scheme, the received signals of different regions for the ith MR can be expressed as

$$\boldsymbol{y}_i = \begin{cases} \sqrt{p_i \beta_i G_{R_i}} \boldsymbol{h}_i^H \boldsymbol{w}_i \boldsymbol{x}_i \\ \quad + \sum\limits_{\substack{j \in [1, N_R] \\ j \neq i}} \sqrt{p_j \beta_j G_{R_j}} \boldsymbol{h}_i^H \boldsymbol{w}_j \boldsymbol{x}_j + \boldsymbol{n}_i, & 0 < s \leq s' \\ \sqrt{p_i \beta_i G_{R_i}} \boldsymbol{h}_i^H \boldsymbol{w}_i \boldsymbol{x}_i + \boldsymbol{n}_i, & s' < s \leq R \end{cases} \tag{1}$$

where s represents the running distance between the first MR and the origin O, p_i is the transmit power for the ith MR, β_i is the large-scale fading of the BS to the ith MR, which is affected by both the path loss and the shadow fading. When the first MR is in the position s, the path loss from the BS to the ith MR expressed as $PL(i)$ can be given by [28]

$$PL(i) = 32.4 + 20 \lg f_c + 20 \lg \sqrt{s_{min}^2 + [s - (i-1)l]^2}, \tag{2}$$

where f_c is the carrier frequency. s_{min} is the shortest distance between the BS and the MR, which can be expressed as

$$s_{min} = \sqrt{d_{min} + (h_{BS} - h_{MR})^2}. \tag{3}$$

β_i can be expressed as

$$\beta_i = 10^{(-PL(i)/10)}. \tag{4}$$

G_{R_i} are the beamforming gains of the receive beam, which can be reflected by beam width [29].

$$G(B_{3dB}, \Delta\theta) = \frac{2\pi}{B_{3dB}} \mathrm{e}^{-4log2(\frac{\Delta\theta}{B_{3dB}})^2}, \tag{5}$$

where B_{3dB} expresses the $3dB$ beam-width and $\Delta\theta$ is the angle difference between the beam main lobe direction and the DOA. The narrower the beam width, the higher the beamforming gain. $\boldsymbol{h}_i$ represents the channel vectors, which can be given by [7]

$$\boldsymbol{h}_i = \alpha_i \mathrm{e}^{\frac{j2\pi s_i}{\lambda}} \sqrt{\frac{2\pi}{B_{3dB}} \mathrm{e}^{-4log2(\frac{\Delta\theta}{B_{3dB}})^2}} \boldsymbol{f}(\phi_i), \tag{6}$$

where α_i obeys the standard normal distribution, s_i indicates the distance from the BS to the ith MR and $\boldsymbol{f}(\phi_i)$ is the array steering vector, which can be expressed as

$$\boldsymbol{f}(\phi_i) = \left[1, \mathrm{e}^{-j2\pi \Delta_T \cos\phi_i}, \ldots, \mathrm{e}^{-j2\pi(N_T-1)\Delta_T \cos\phi_i}\right]^H. \tag{7}$$

$\boldsymbol{w}_i$ is the beamforming weight vector, which can be derived based on the DOA method [30].

$$\boldsymbol{w}_i = \frac{1}{\sqrt{N_T}} \left[1, \mathrm{e}^{-j2\pi \Delta_T \cos\phi_i}, \ldots, \mathrm{e}^{-j2\pi(N_T-1)\Delta_T \cos\phi_i}\right]^H. \tag{8}$$

P is the total power transmitted by the BS. The transmit power p_i for ith MR can be obtained by waterfilling [31]

$$p_i = (\frac{1}{\mu} - \frac{\sigma_n^2}{\beta_i |\boldsymbol{h}_i^H \boldsymbol{w}_i|^2})^+, \tag{9}$$

where $(x)^+ = max(x, 0)$, σ_n^2 is the noise power, $1/\mu$ is the water level satisfying

$$\sum (\frac{1}{\mu} - \frac{\sigma_n^2}{\beta_i |\boldsymbol{h}_i^H \boldsymbol{w}_i|^2}) = P. \tag{10}$$

$\boldsymbol{x}_i$ denotes the transmitted signal aimed at the ith MR in the condition of $\mathbb{E}\{|x_i|\} = 1$,where $\mathbb{E}\{\cdot\}$ indicates mathematical expectations. The $\boldsymbol{n}_i$ is the additive white Gaussian noise (AWGN), which follows normal distribution with mean 0 and variance σ_n^2.

The correlation of the steering vector is defined as the IBA, which can be expressed as

$$\rho = \frac{|\boldsymbol{f}(\phi_i)^H \boldsymbol{f}(\phi_j)|}{N_T}, \quad i, j \in [1, N_R],\ i \neq j. \tag{11}$$

(7) is put into (11) for further calculation, (12) can be obtained.

$$\begin{aligned} \rho &= \frac{1}{N_T} \left| \sum_{n=0}^{N_T-1} \mathrm{e}^{j2\pi \Delta_T (\cos\phi_i - \cos\phi_j) n} \right| \\ &= \frac{1}{N_T} \left| \frac{1 - \mathrm{e}^{j} 2\pi \Delta_T (\cos\phi_i - \cos\phi_j) N_T}{1 - \mathrm{e}^{j} 2\pi \Delta_T (\cos\phi_i - \cos\phi_j)} \right|, \\ & i, j \in [1, N_R], \quad i \neq j. \end{aligned} \tag{12}$$

For the sake of ensuring the independence between beams, it is necessary to meet the requirement of angular resolution. The angular interval of any two adjacent MRs should be greater than or equal to $1/N_T \Delta_T$, i.e.,

$$|cos(\phi_i) - cos(\phi_{i+1})| \geq \frac{1}{N_T \Delta_T}, i \in [1, N_R - 1], \tag{13}$$

where ϕ_i and ϕ_{i+1} indicate the DOAs from the BS to the ith and $i+1$th MRs, respectively. From Fig.1, $cos(\phi_i)$ and $cos(\phi_{i+1})$ can be denoted as

$$\begin{cases} \cos(\phi_i) = \dfrac{s - (i-1)l}{\sqrt{{s_{min}}^2 + [s - (i-1)l]^2}} & \text{(14a)} \\ \cos(\phi_{i+1}) = \dfrac{s - il}{\sqrt{{s_{min}}^2 + [s - il]^2}} & \text{(14b)} \end{cases}$$

Substituting (14a) and (14b) into (13) gives

$$\left| \frac{s-(i-1)l}{\sqrt{{s_{min}}^2 + [s-(i-1)l]^2}} - \frac{s - il}{\sqrt{{s_{min}}^2 + [s - il]^2}} \right| \geq \frac{1}{N_T \Delta_T}. \tag{15}$$

As shown in Fig. 3, ρ is not a monotonic function of s. As the distance between the coordinate origin O and the first MR increases, the IBA experiences ups and downs and then increases dramatically after the train arrives at a certain location. From that position, multi-stream beamforming is no longer suitable because the interference inter multiple beams has a greater impact on the performance than the gain of multiple beams.

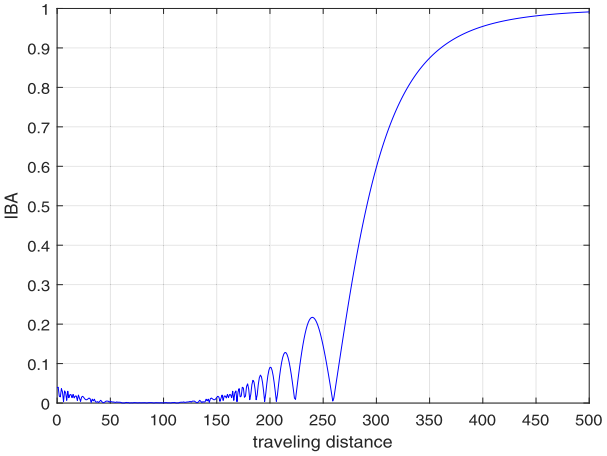

FIGURE 3. IBA with the traveling distance.

To get the beam switching position, the angular resolution of any two adjacent beams needs to be calculated. However, calculating which angular resolution between the two beams needs to be considered. It can be proved from the theoretical derivation that the angular resolution varies with the index of the MR. Therefore, the expression on the left side of (13) is derived for i, we have

$$\frac{\mathrm{d}|\cos(\phi_i) - \cos(\phi_{i+1})|}{\mathrm{d}i}. \tag{16}$$

When the train moves to the edge of the BS, it can be considered that all DOAs belong to $[0, \pi/2]$. So (16) can be further written as

$$\begin{aligned} &\frac{\mathrm{d}|\cos(\phi_i) - \cos(\phi_{i+1})|}{\mathrm{d}i} \\ &= \frac{\mathrm{d}\cos(\phi_i)}{\mathrm{d}i} - \frac{\mathrm{d}\cos(\phi_{i+1})}{\mathrm{d}i}, \\ &\phi_i, \phi_{i+1} \in [0, \pi/2], \quad \phi_{i+1} > \phi_i. \end{aligned} \tag{17}$$

According to (14a), the derivative of $\cos(\phi_i)$ relative to the variable i can be calculated as

$$\begin{aligned} \frac{\mathrm{d}\cos(\phi_i)}{\mathrm{d}i} &= \frac{\mathrm{d}}{\mathrm{d}i} \left(\frac{s - (i-1)l}{\sqrt{{s_{min}}^2 + [s - (i-1)l]^2}} \right) \\ &= \frac{-lS_h - [s - (i-1)l]^2 \left(S_h^2\right)^{-\frac{1}{2}} (-l)}{S_h^2} \\ &= \frac{-l}{S_h} \frac{S_h - [s - (i-1)l]^2 S_h^{-1}}{S_h} \\ &= \frac{-l}{S_h} \left\{ 1 - \frac{[s - (i-1)l]^2}{S_h^2} \right\}, \end{aligned} \tag{18}$$

where S_h is expressed as

$$S_h = \sqrt{{s_{min}}^2 + [s - (i-1)l]^2}. \tag{19}$$

According to (14a) and (19), we have

$$\cos(\phi_i) = \frac{s-(i-1)l}{\sqrt{{s_{min}}^2 + [s-(i-1)l]^2}} = \frac{s-(i-1)l}{S_h}. \quad (20)$$

According to (20), (18) can be further simplified as

$$\begin{aligned}\frac{\mathrm{d}\cos(\phi_i)}{\mathrm{d}i} &= \frac{-l}{S_h}\left[1-\cos^2(\phi_i)\right] \\ &= \frac{-l}{S_h}\sin^2(\phi_i). \end{aligned} \quad (21)$$

From Fig. 1, we can get a relational expression:

$$\sin(\phi_i) = \frac{s_{min}}{\sqrt{{s_{min}}^2 + [s-(i-1)l]^2}} = \frac{s_{min}}{S_h}. \quad (22)$$

Convenient for analysis, for (21), the numerator and the denominator are multiplied by s_{min} at the same time, then substituting (22), we have

$$\begin{aligned}\frac{\mathrm{d}\cos(\phi_i)}{\mathrm{d}i} &= \frac{-ls_{min}}{S_h s_{min}}\sin^2(\phi_i) \\ &= \frac{-l}{s_{min}}\frac{s_{min}}{S_h}\sin^2(\phi_i) \\ &= \frac{-l}{s_{min}}\sin^3(\phi_i). \end{aligned} \quad (23)$$

Similarly, then we have

$$\begin{aligned}\frac{\mathrm{d}\cos(\phi_{i+1})}{\mathrm{d}i} &= \frac{\mathrm{d}}{\mathrm{d}i}\left(\frac{s-il}{\sqrt{{s_{min}}^2 + [s-il]^2}}\right) \\ &= \frac{-l}{s_{min}}\sin^3(\phi_{i+1}), \end{aligned} \quad (24)$$

where

$$\sin(\phi_{i+1}) = \frac{s_{min}}{\sqrt{{s_{min}}^2 + [s-il]^2}}. \quad (25)$$

Substituting (23) and (24) into (17) is simplified as

$$\begin{aligned}&\frac{\mathrm{d}|\cos(\phi_i)-\cos(\phi_{i+1})|}{\mathrm{d}i} \\ &= \frac{l}{s_{min}}\left[\sin^3(\phi_{i+1})-\sin^3(\phi_i)\right] \\ &> 0, \phi_i, \phi_{i+1} \in [0, \pi/2], \quad \phi_{i+1} > \phi_i. \end{aligned} \quad (26)$$

From the mathematical derivation, the equation (26) is greater than zero when all DOAs belong to $[0, \pi/2]$, so that the left expression of (13) is monotonically increasing with respect to i. That is to say, as the index of the MR increases, the angular resolution inter the beams increases. As can be seen from the simulation of Fig. 4, the angular resolution expression is a monotonically increasing function with respect to the index i of the MR.

It can be seen from the above analysis that the smaller the angular resolution between the beams, the greater the IBA between the beams. For the proposed scheme, the optimal switching point s' is a key parameter that determines the working state of the activated multiple beams. The size of s' can be obtained by calculating the angular resolution between

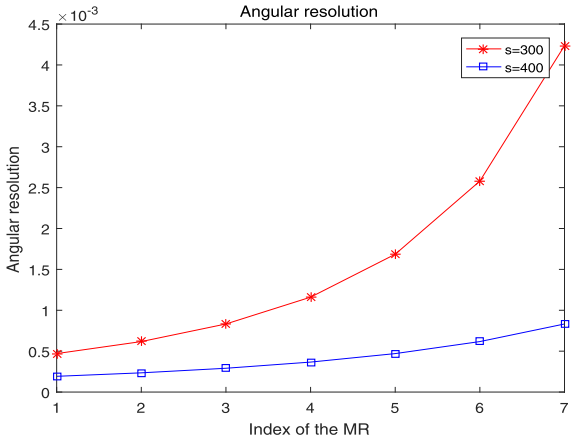

FIGURE 4. Angular resolution with the index *i* of the MR.

any two adjacent beams, that is, the expression on the left side of inequality (15) takes an equal sign. As the train travels towards the edge of the cell, the index of the MR increases in the opposite direction of speed. Based on the above mathematical analysis, the optimal switching point may be obtained in three cases: calculating the angular resolution of the first two beams, the middle two beams or the last two beams.

As the train travels, the first two beams cannot tolerate the IBA initially. If the beam switching is performed at the location where the first two beams cannot tolerate the IBA and other beams can tolerate the IBA, which may reduce the throughput of the system due to the performance loss. If the beam switching is performed at the position where the last two beams cannot tolerate the IBA and all the previous beams are already intolerable, which causes a large error rate and undoubtedly degrades the performance of the system. When the beam switching is performed at the position where the middle two beams cannot tolerate the IBA, that is, the IBA which is not tolerated between the preceding beams can be tolerated between the subsequent beams at this position, which can achieve a tradeoff between the performance and the interference. Therefore, the beam switching position can be determined by calculating the angular resolution of the middle two beams.

According to the above analysis, two adjacent beams are qualitatively selected. In order to further determine the optimal switching point, we find the first-order partial derivative of (26), which can be expressed as follows.

$$\begin{aligned}&\frac{\mathrm{d}^2|\cos(\phi_i)-\cos(\phi_{i+1})|}{\mathrm{d}i^2} \\ &= \frac{l}{s_{min}}\frac{\mathrm{d}\left[\sin^3(\phi_{i+1})-\sin^3(\phi_i)\right]}{\mathrm{d}i}, \\ &\phi_i, \phi_{i+1} \in [0, \pi/2], \quad \phi_{i+1} > \phi_i, \end{aligned} \quad (27)$$

where

$$\frac{\mathrm{d}\sin^3(\phi_i)}{\mathrm{d}i} = \frac{\mathrm{d}}{\mathrm{d}i}\left\{\frac{s_{min}^3}{\left[s_{min}^2 + [s-(i-1)l]^2\right]^{\frac{3}{2}}}\right\}$$

TABLE 1. Values of s_i' and s_i for any two adjacent beams.

the index i of MR	s_i'(m)	s_i(m)	$s_i' - s_i$
1	184	-2.0609	186.0609
2	209	22.9391	186.0609
3	234	77.0609	156.9391
4	259	102.0609	156.9391
5	284	97.9391	186.0609
6	309	122.9391	186.0609
7	334	null	null

$$
\begin{aligned}
&= -3ls_{min}^3 S_h^{-5}\left[s-(i-1)l\right] \\
&= -3l\frac{s_{min}^3}{S_h^3}\frac{s-(i-1)l}{S_h}\frac{s_{min}}{S_h}\frac{1}{s_{min}} \\
&= -\frac{3l}{s_{min}}\cos(\phi_i)\sin^4(\phi_i). \qquad (28)
\end{aligned}
$$

Similarly, we have

$$
\frac{\mathrm{d}\sin^3\phi_{i+1}}{\mathrm{d}i} = -\frac{3l}{s_{min}}\cos(\phi_{i+1})\sin^4(\phi_{i+1}). \qquad (29)
$$

Substituting (28) and (29) into (27) is simplified as

$$
\begin{aligned}
&\frac{\mathrm{d}^2|\cos(\phi_i)-\cos(\phi_{i+1})|}{\mathrm{d}i^2} \\
&= \frac{3l^2}{s_{min}^2}\Big[\cos(\phi_i)\sin^4(\phi_i) \\
&\qquad - \cos(\phi_{i+1})\sin^4(\phi_{i+1})\Big], \quad i\in[1,N_R-1]. \qquad (30)
\end{aligned}
$$

Let (30) be equal to 0, the index i of MR and the corresponding position s_i can be obtained. s_i is the theoretical optimal switching point based on the optimal adjacent two beams. Taking equal sign for (15), the index i of the MR and the corresponding switching position s_i' can be obtained. Taking the same index of MR, the shortest distance of $s_i' - s_i$ can be calculated, which will be used as the basis for the selection of adjacent two beams. Taking $i \in [1, 7]$ as an example, the specific values are listed in Table 1.

It can be seen from Table 1 that the distance difference is the same when i is 3 and 4. It is known from the first-order partial derivative of (15) that the angular resolution between beams increases with i. When making a choice between $i = 3$ and $i = 4$, the points near the middle are more likely to be selected. Therefore, we choose $i = 4$, that is, calculating the middle two beams get the optimal switching point.

B. DESCRIPTION OF THE PROPOSED BEAM SELECTION ALGORITHM

In this section, the algorithm of the proposed scheme is described, and the algorithm steps are as follows.

Step 1. According to (15), the switching position s' of the middle two beams satisfying the angular resolution requirements is calculated.

Step 2. Taking step length of m meters, the program is executed at a point every m meters in the coverage area R of the BS, and a total of $M = R/m$ points need to be performed.

Step 3. All beams are activated for serving all MRs before reaching the switching point. Therefore, it is judged whether the train arrives at the switching point s'. If the train has not yet reached the switching point s', the throughput of the N_R beams is calculated at each point and summed to the total throughput of the system. This process is performed until the switching point is reached.

Step 4. Only one optimal beam is activated to serve one MR after reaching the switching point. The throughput of the N_R beams is calculated at each point, and then one of the beams with the highest throughput is selected as the transmit beam.

The flow of the proposed algorithm is listed in Algorithm 2.

Algorithm 2 Low Complexity Beam Selection Algorithm

Input:
Get the switching point s'

for s = 0:10:R **do**
  if s < s' **then**
    All beams are activated to serve all MRs
    $B_{opt} = \{1, 2, \ldots, N_R\}$
    $C = \sum_{i\in[1,N_R]} B\log_2(1 + SINR_i)$
  else
    $C = \max_{i\in[1,N_R]} B\log_2(1 + SINR_i)$
    The index of the optimal activated beam is returned,
    i.e.:$B_{opt} = Index \max_{i\in[1,N_R]} C$
  end if
end for
return C, B_{opt}

C. COMPUTATIONAL COMPLEXITY OF THE PROPOSED BEAM SELECTION ALGORITHM

In this section, a complexity analysis is performed. The analysis proves that the complexity of the proposed scheme is much lower than that of the traversal searching algorithm.

It is assumed that every m meters is calculated once within the coverage radius R of one BS, then $M = R/m$ times need to be calculated, and there are a total of N_R MRs and N_b beams.

1) FOR THE CASE OF $N_R = N_b$

For the traversal searching algorithm, the computational complexity is

$$
f_{previous} = [N_R + (N_R - 1) + \ldots + 1]M = \frac{N_R(N_R+1)}{2}M. \qquad (31)
$$

In contrast, for the proposed method of finding the working state of the activated multiple beams, the computational complexity is

$$
f_{proposed} \le N_R M. \qquad (32)
$$

Comparing the computational complexities of the two schemes by (31) and (32), then we have

$$
\frac{f_{previous}}{f_{proposed}} \ge \frac{N_R+1}{2}. \qquad (33)
$$

TABLE 2. Parameter settings.

Parameters	Values
Number of BS antenna elements N_T	1024
Number of MRs N_R	8
Carrier frequency f_c	38GHz
Bandwidth B	1GHz
Coverage radius R	500m
Length of train l_T	200m
Length of adjacent MRs l	25m
distance between BS and the track d_{min}	20m
Height of BS h_{BS}	10m
Height of MRs h_{MR}	3m
Train velocity v	360km/h
Transmit power P	30dBm
Normalized antenna element spacing Δ_T	0.5
Noise power N_0	-174dBm/Hz
The threshold of the SINR γ_{th}	10dBm

2) FOR THE CASE OF $N_R > N_b$

For the traversal searching algorithm, the computational complexity is

$$f_{previous} = [N_R(N_R-1)\ldots(N_R-N_b+1)]\,M. \quad (34)$$

For the proposed scheme, it is only necessary to select N_b MRs from the N_R MRs as receivers before the train reaches the switching point, and the computational complexity is

$$f_{proposed} = \binom{N_b}{N_R} M = \frac{N_R(N_R-1)\ldots(N_R-N_b+1)}{N_b!} M. \quad (35)$$

The complexities of the two schemes are compared according to (34) and (35), then we have

$$\frac{f_{previous}}{f_{proposed}} = N_b!. \quad (36)$$

Obviously, the number of MRs and beams is greater than or equal to one, so (33) and (36) are always greater than one. That is to say, the computational complexity of the proposed scheme is lower than that of the previous traversal searching algorithm. Moreover, as the number of MRs and beams increases, the proposed scheme can greatly reduce the computational complexity in contrast to the traversal searching algorithm.

V. PERFORMANCE SIMULATION

In this section, numerical simulations were given to evaluate the proposed scheme in reducing system complexity while maintaining throughput. The basic comparison is with previous scheme in which the traversal searching algorithm is used to find the optimal activated beam set to maximize system throughput. In the proposed scheme, predictable train position information and angular resolution between beams are utilized to determine whether to activate all beams or to activate only one beam. The simulation parameter settings are shown in Table 2.

Considering that the switching point is determined by the system parameters, the influence of the system parameters such as s_{min}, l, N_T, Δ_T on the switching point s' is simulated as follows.

TABLE 3. The effect of s_{min} on the switching point s'.

s_{min}(m)	15	20	25
s'(m)	229	259	286

TABLE 4. The effect of l on the switching point s'.

l(m)	20	25	30	35	40
s'(m)	229	259	287	315	341

TABLE 5. The effect of N_T on the switching point s'.

N_T	128	256	512	1024
s'(m)	172	195	223	259

TABLE 6. The effect of N_T on the switching point s'.

Δ_T	0.3	0.4	0.5	0.6
s'(m)	232	246	259	270

The values of the switching points under different s_{min} are listed in Table 3. As the distance between the train and the MR increases, the angular resolution inter beams becomes larger, and the tolerance of the inter beam ambiguity increases. Therefore, the beam switching s' becomes larger.

The change of s' with l is shown in Table 4. The interference between the beams is reduced as the distance between adjacent MRs increases. Thus, the switching point is getting farther and farther.

It can be seen from Table 5 that as N_T increases, s' increases. The more the number of antenna elements, the greater the gain of beamforming. Since the benefit of multi-beam gain is greater than the interference between multiple beams, the beam switching point s' becomes larger.

The values of the switching points under different Δ_T are displayed in Table 6. The larger the antenna element spacing Δ_T, the lower the spatial correlation and the smaller the interference between multiple beams. Therefore, the beam switching point is farther and farther.

The received signal to inference and noise ratio (SINR) of different regions for the ith MR can be expressed as

$$SINR_i = \begin{cases} \dfrac{\mathbb{E}\left\{\left|\sqrt{p_i\beta_i G_{R_i}}\boldsymbol{h}_i^H\boldsymbol{w}_i\boldsymbol{x}_i\right|^2\right\}}{\mathbb{E}\left\{\left|\sum\limits_{\substack{j\in[1,N_R]\\ j\neq i}}\sqrt{p_j\beta_j G_{R_j}}\boldsymbol{h}_i^H\boldsymbol{w}_j\boldsymbol{x}_j+\boldsymbol{n}_i\right|^2\right\}} \\ = \dfrac{\left|\sqrt{p_i\beta_i G_{R_i}}\boldsymbol{h}_i^H\boldsymbol{w}_i\right|^2}{\sum\limits_{\substack{j\in[1,N_R]\\ j\neq i}}\left|\sqrt{p_j\beta_j G_{R_j}}\boldsymbol{h}_i^H\boldsymbol{w}_j\right|^2+\sigma_n^2}, & 0<s\le s' \\ \dfrac{\mathbb{E}\left\{\left|\sqrt{p_i\beta_i G_{R_i}}\boldsymbol{h}_i^H\boldsymbol{w}_i\boldsymbol{x}_i\right|^2\right\}}{\mathbb{E}\left\{|\boldsymbol{n}_i|^2\right\}} \\ = \dfrac{\left|\sqrt{p_i\beta_i G_{R_i}}\boldsymbol{h}_i^H\boldsymbol{w}_i\right|^2}{\sigma_n^2}, & s'<s\le R \end{cases} \quad (37)$$

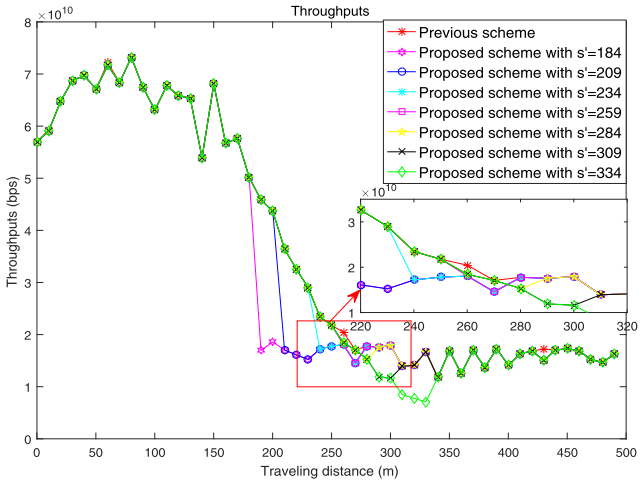

FIGURE 5. Throughputs of different switching points.

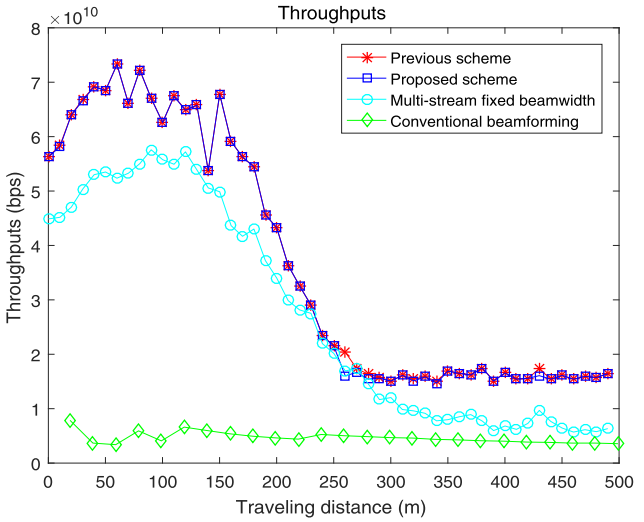

FIGURE 6. Throughputs of different switching points.

Then the throughput of the HSR system is given by

$$C = \begin{cases} \sum\limits_{i\in[1,N_R]} B\log_2(1+SINR_i), & 0 < s \le s' \\ \max\limits_{i\in[1,N_R]} B\log_2(1+SINR_i), & s' < s \le R \end{cases} \tag{38}$$

Fig. 5 describes the throughputs of the previous scheme and the proposed scheme with different beam switching position s'. Before 259 meters, the gain of multi-beamforming is greater than the interference inter the multiple beams. Therefore, beam switching is performed before 259 meters, which will bring performance loss because the optimal switching position has not yet been reached. After 259 meters, the interference inter the multiple beams is greater than the gain of the multi-beamforming. Thus, the throughput of the system is reduced when the beam switching is performed after 259 meters, because the switching position is later than the optimal switching position. In order to see more clearly, the part of $s \in [220, 320]$ in the Fig. 5 is enlarged. When $s' = 259$, the curve of the proposed scheme almost coincides with the previous scheme, which means that there is almost no loss of performance.

Fig. 6 illustrates the throughputs of the previous scheme, multi-stream beamforming with fixed beamwidth, conventional beamforming and proposed scheme. For the conventional beamforming, the signal is transmitted by a single beam of the BS with fixed beamwidth whose transmit beamforming gain remains almost unchanged. The throughput of single beamforming is at a low level and gradually decreases but does not drop rapidly. In contrast to the conventional beamforming, the throughput of multi-stream beamforming with fixed beamwidth is greatly affected by the train position and rapidly decreases as the distance between the BS and MR increases. The reason is that there is interference inter multiple beams and the interference is getting larger and larger when the train runs over 270m. In the previous scheme, both the BS and the MR are equipped with large-scale antenna arrays. The BS can simultaneously form multiple beams with

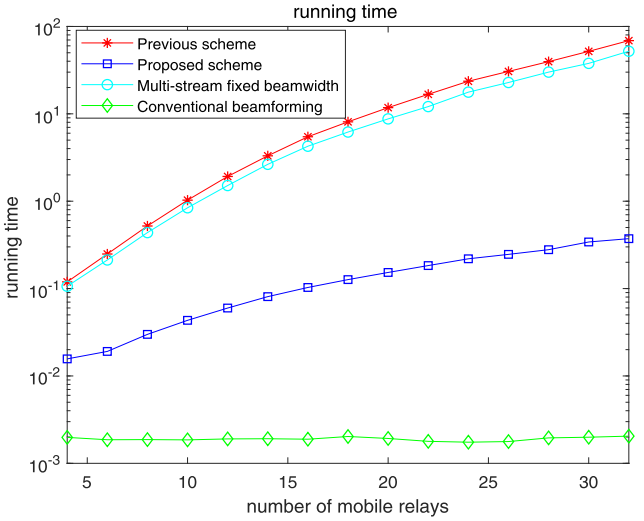

FIGURE 7. Running time comparison.

different beam widths to transmit signals, and the MR can form a receiving beam to automatically adjust the receiving direction. The throughput of this scheme will be greatly improved. For the proposed scheme, all beams are activated before the switching point and only one beam is activated after the switching point. The curve of the proposed scheme with a switching point of 259m is almost coincident to the previous scheme, which means that the performance loss in the proposed scheme can be neglected.

Fig. 7 compares the online running time of the proposed scheme and the previous scheme, multi-stream beamforming with fixed beamwidth, conventional beamforming and proposed scheme. In the previous scheme and multi-stream beamforming scheme with fixed beamwidth, the adaptive beam adjusting algorithm was adopted, and the throughput of the system was maximized by the continuously searching the beams. Therefore, the running time of the two schemes

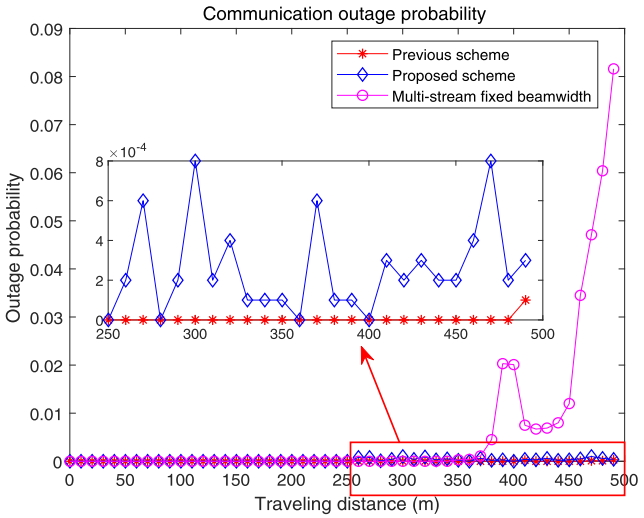

FIGURE 8. Communication outage probability comparison.

is almost the same. Furthermore, as the number of MRs increases, this traversal searching algorithm will greatly increase the complexity of the system and is detrimental to real-time applications. For the conventional beamforming scheme, it does not have the traversal searching process. Therefore, the running time is short. However, this scheme always uses only one beam to transmit signals, and the throughput of the system is very low. In the proposed scheme, the position of the middle two beams that cannot tolerate the IBA can be calculated offline as the beam switching position according to the requirements of the angular resolution. In the running of the train from the center of the cell to the edge of the cell, all beams are employed to transmit signals at the beginning, and when the train reaches the switching position, only one optimal beam is activated. Although the proposed scheme has longer running time than the conventional beamforming scheme, the actual running time is shorter, which can satisfy the real-time processing of the algorithm. Compared with the previous scheme, the proposed scheme has almost the same throughput and shorter running time.

For multi-beamforming methods, the communication outage probability is defined as [21]

$$P_{out} = \begin{cases} \prod\limits_{i\in[1,N_R]} P(SINR_i < \gamma_{th}), & 0 < s \le s' \\ P(\max\limits_{i\in[1,N_R]} (SINR_i) < \gamma_{th}), & s' < s \le R \end{cases} \tag{39}$$

where γ_{th} represents the threshold of the SINR.

Fig. 8 describes the communication outage probabilities of the previous scheme, the multi-stream beamforming scheme with fixed beamwidth and the proposed scheme. Before reaching the switching point, all three schemes use multiple beams to transmit signals. The communication interruption will occur when the SINR of all beams is less than the threshold of the SINR. Therefore, the probability of communication interruption basically remains at zero when multiple beams are employed. In the multi-stream beamforming scheme with fixed beamwidth, the BS uses one beam for transmission when the interference inter multiple beams is larger than the gain inter multiple beams in the cell edge region. However, the beamwidth at that point cannot provide sufficiently high transmit gain to counter the path loss, thus affecting communication. Therefore, it has a high probability of interruption when $s \in [350, 500]$. In contrast, the proposed scheme and the previous scheme with variable width beams have communication outage probability of almost zero. To more clearly see the outage probabilities of the two schemes after reaching the switching point, this part is shown enlarged in Fig. 8. Since the two schemes have different activated beam numbers in rare cases, the communication outage probabilities of the two schemes are different. As can be seen from Fig. 8, the proposed scheme has a slightly higher probability of interruption than the previous scheme at certain points.

VI. CONCLUSION

In order to improve the system throughput while reducing the complexity of system implementation, a low-complexity beam selection scheme for HSR communication systems based on massive MIMO is proposed in this paper. In the proposed scheme, the working state of the activated multiple beams is divided into two kinds: one is that all beams are activated to serve all MRs in the vicinity of the BS, and the other is that only one beam is activated to serve one MR in the cell edge area. The optimal working state is determined by the optimal switching point. The beam switching point is determined by calculating the angle resolution of the intermediate two beams. Analysis and simulation show that the proposed scheme has little difference in throughput performance from the previous scheme and reduces the complexity of the system.

The low-complexity beam selection scheme for HSR communication systems proposed in this paper can be future studied. After reaching the switching point, how to reduce inter-beam interference while still using multiple beams, such as assigning different frequency bands to multiple beams, is our future research work.

REFERENCES

[1] X. Liu and D. Qiao, "Location-fair beamforming for high speed railway communication systems," *IEEE Access*, vol. 6, pp. 28632–28642, 2018.

[2] R. He, B. Ai, G. Wang, K. Guan, Z. Zhong, A. F. Molisch, C. Briso-Rodriguez, and C. P. Oestges, "High-speed railway communications: From GSM-R to LTE-R," *IEEE Veh. Technol. Mag.*, vol. 11, no. 3, pp. 49–58, Sep. 2016.

[3] W. Roh, J.-Y. Seol, J. Park, B. Lee, J. Lee, Y. Kim, J. Cho, K. Cheun, and F. Aryanfar, "Millimeter-wave beamforming as an enabling technology for 5G cellular communications: Theoretical feasibility and prototype results," *IEEE Commun. Mag.*, vol. 52, no. 2, pp. 106–113, Feb. 2014.

[4] Y. Cui, X. Fang, and L. Yan, "Hybrid spatial modulation beamforming for mmWave railway communication systems," *IEEE Trans. Veh. Technol.*, vol. 65, no. 12, pp. 9597–9606, Dec. 2016.

[5] X. Chen, J. Lu, T. Li, P. Fan, and K. B. Letaief, "Directivity-Beamwidth tradeoff of massive MIMO uplink beamforming for high speed train communication," *IEEE Access*, vol. 5, pp. 5936–5946, 2017.

[6] E. G. Larsson, O. Edfors, F. Tufvesson, and T. L. Marzetta, "Massive MIMO for next generation wireless systems," *IEEE Commun. Mag.*, vol. 52, no. 2, pp. 186–195, Feb. 2014.

[7] D. Tse and P. Viswanath, *Fundamentals of Wireless Communication*. Cambridge, U.K.: Cambridge Univ. Press, 2005.
[8] P. Fan, J. Zhao, and C.-L. I, "5G high mobility wireless communications: Challenges and solutions," *China Commun.*, vol. 13, no. 2, pp. 1–13, 2016.
[9] W. Zhou, J. Wu, and P. Fan, "Spectral efficient Doppler diversity transmissions in high mobility systems with channel estimation errors," in *Proc. IEEE 81st Veh. Technol. Conf. (VTC Spring)*, May 2015, pp. 1–6.
[10] M. A. Mahamadu, J. Wu, Z. Ma, W. Zhou, Y. Tang, and P. Fan, "Fundamental tradeoff between Doppler diversity and channel estimation errors in SIMO high mobility communication systems," *IEEE Access*, vol. 6, pp. 21867–21878, 2018.
[11] W. Zhou, J. Wu, and P. Fan, "High mobility wireless communications with Doppler diversity: Fundamental performance limits," *IEEE Trans. Wireless Commun.*, vol. 14, no. 12, pp. 6981–6992, Dec. 2015.
[12] J. Zhao, Y. Liu, Y. Gong, C. Wang, and L. Fan, "A dual-link soft handover scheme for C/U plane split network in high-speed railway," *IEEE Access*, vol. 6, pp. 12473–12482, 2018.
[13] Q. Wang, G. Ren, and J. Tu, "A soft handover algorithm for TD-LTE system in high-speed railway scenario," in *Proc. IEEE Int. Conf. Signal Process., Commun. Comput. (ICSPCC)*, Sep. 2011, pp. 1–4.
[14] S. Xie, X. Yu, and Y. Luo, "A seamless dual-link handover scheme with optimized threshold for C/U plane network in high-speed rail," in *Proc. IEEE 83rd Veh. Technol. Conf. (VTC Spring)*, May 2016, pp. 1–5.
[15] L. Tian, J. Li, Y. Huang, J. Shi, and J. Zhou, "Seamless dual-link handover scheme in broadband wireless communication systems for high-speed rail," *IEEE J. Sel. Areas Commun.*, vol. 30, no. 4, pp. 708–718, May 2012.
[16] L. Zhang, H. Xiong, and X. Dai, "A new channel estimation algorithm for fast linear-time-varying channel in MIMO-OFDM systems," in *Proc. IEEE 18th Int. Conf. Commun. Technol. (ICCT)*, Oct. 2018, pp. 155–158.
[17] L. Zhu, F. R. Yu, B. Ning, and T. Tang, "Communication-based train control (CBTC) systems with cooperative relaying: Design and performance analysis," *IEEE Trans. Veh. Technol.*, vol. 63, no. 5, pp. 2162–2172, Jun. 2014.
[18] K. Xiong, B. Wang, C. Jiang, and K. J. R. Liu, "A broad beamforming approach for high-mobility communications," *IEEE Trans. Veh. Technol.*, vol. 66, no. 11, pp. 10546–10550, Nov. 2017.
[19] M. Gao, B. Ai, Y. Niu, Z. Zhong, Y. Liu, G. Ma, Z. Zhang, and D. Li, "Dynamic mmWave beam tracking for high speed railway communications," in *Proc. IEEE Wireless Commun. Netw. Conf. Workshops (WCNCW)*, Apr. 2018, pp. 278–283.
[20] X. Chen, J. Lu, S. Liu, and P. Fan, "Location-aided umbrella-shaped massive MIMO beamforming scheme with transmit diversity for high speed railway communications," in *Proc. IEEE 83rd Veh. Technol. Conf. (VTC Spring)*, May 2016, pp. 1–5.
[21] Y. Cui, X. Fang, Y. Fang, and M. Xiao, "Optimal nonuniform steady mmWave beamforming for high-speed railway," *IEEE Trans. Veh. Technol.*, vol. 67, no. 5, pp. 4350–4358, May 2018.
[22] L. Yan, X. Fang, and Y. Fang, "Stable beamforming with low overhead for C/U-plane decoupled HSR wireless networks," *IEEE Trans. Veh. Technol.*, vol. 67, no. 7, pp. 6075–6086, Jul. 2018.
[23] J. Wang, H. Zhu, L. Dai, N. J. Gomes, and J. Wang, "Low-complexity beam allocation for switched-beam based multiuser massive MIMO systems," *IEEE Trans. Wireless Commun.*, vol. 15, no. 12, pp. 8236–8248, Dec. 2016.
[24] J. Wang, H. Zhu, N. J. Gomes, and J. Wang, "Frequency reuse of beam allocation for multiuser massive MIMO systems," *IEEE Trans. Wireless Commun.*, vol. 17, no. 4, pp. 2346–2359, Apr. 2018.
[25] H. Yin, R. Jiang, and Y. Xu, "An mmWave-based adaptive multi-beamforming scheme for high speed railway communications," in *Proc. 10th Int. Conf. Wireless Commun. Signal Process. (WCSP)*, Oct. 2018, pp. 1–6.
[26] W. Luo, X. Fang, M. Cheng, and Y. Zhao, "Efficient multiple-group multiple-antenna (MGMA) scheme for high-speed railway viaducts," *IEEE Trans. Veh. Technol.*, vol. 62, no. 6, pp. 2558–2569, Jul. 2013.
[27] J. Kim and I. G. Kim, "Distributed antenna system-based millimeter-wave mobile broadband communication system for high speed trains," in *Proc. Int. Conf. ICT Converg. (ICTC)*, Oct. 2013, pp. 218–222.
[28] M. Marcus and B. Pattan, "Millimeter wave propagation: Spectrum management implications," *IEEE Microw.*, vol. 6, no. 2, pp. 54–62, Jun. 2005.
[29] V. Vakilian, J.-F. Frigon, and S. Roy, "Effects of angle-of-arrival estimation errors, angular spread and antenna beamwidth on the performance of reconfigurable SISO systems," in *Proc. IEEE Pacific Rim Conf. Commun., Comput. Signal Process.*, Aug. 2011, pp. 515–519.
[30] C. Balanis, *Antenna Theory: Analysis and Design*. Hoboken, NJ, USA: Wiley, 2012.
[31] S. Huang, H. Yin, H. Li, and V. C. M. Leung, "Decremental user selection for large-scale multi-user MIMO downlink with zero-forcing beamforming," *IEEE Wireless Commun. Lett.*, vol. 1, no. 5, pp. 480–483, Oct. 2012.

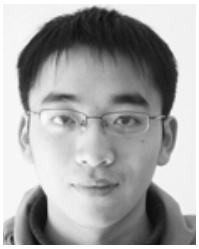

RUI JIANG was born in Jiangsu, China, in 1985. He received the B.S. and Ph.D. degrees in electronic engineering from the Nanjing University of Aeronautics and Astronautics (NUAA), Nanjing, China, in 2007 and 2013, respectively. In 2013, he joined the Department of Telecommunications and Information Engineering, Nanjing University of Posts and Telecommunications (NJUPT), Nanjing, where he is currently an Associate Professor. His research focuses on wireless communications.

JIAQI ZHAO received the B.E. degree in communication engineering from China Jiliang University, Hangzhou, China, in 2018. She is currently pursuing the master's degree with the Nanjing University of Posts and Telecommunications (NJUPT), Nanjing, China. Her research interests include high-speed railway communications and beamforming.

YOUYUN XU (Senior Member, IEEE) received the Ph.D. degree in information and communication engineering from Shanghai Jiao Tong University (SJTU), China, in 1999. He is currently a Professor with the Nanjing University of Posts and Telecommunications. He is also a part-time Professor with the Institute of Wireless Communication Technologies, SJTU. He has over 20-year professional experience of teaching and researching in communication theory and engineering with research and development achievement, such as the WCDMA Trial System under C3G Framework in China, in 1999, the B3G-TDD Trial System under FuTURE Framework in China, in 2006, and the Chinese Digital TV Broadcasting System. His current research interests include new-generation wireless mobile communication systems (LTE, IM-T Advanced, and related), advanced channel coding and modulation techniques, multiuser information theory and radio resource management, wireless sensor networks, and cognitive radio networks. He is a Senior Member of the Chinese Institute of Electronics and a member of IEICE.

XIAOMING WANG (Member, IEEE) received the Ph.D. degree in information and communication engineering from the National Mobile Communications Research Laboratory, Southeast University, Nanjing, China, in 2016.

He is currently a Lecturer with the Nanjing University of Posts and Telecommunications (NJUPT), Nanjing. His research interests include radio resource management, green communications, and machine learning in communications.

LI ZHANG received the B.S. degree from the Changsha University of Science and Technology, in 2007, and the M.S. and Ph.D. degrees from the Nanjing University of Aeronautics and Astronautics, in 2010 and 2015, respectively. He joined the College of Computer Science and Technology, Nanjing Forestry University, as a Lecturer, in 2016. His current research interests include machine learning and high-speed railway communications.